JACS
JOURNAL OF THE AMERICAN CHEMICAL SOCIETY

ARTICLE

pubs.acs.org/JACS

Hydrosilylation with Biscarbene Rh(I) Complexes: Experimental Evidence for a Silylene-Based Mechanism

Peter Gigler,[†,‡] Bettina Bechlars,[‡] Wolfgang A. Herrmann,[*,‡] and Fritz E. Kühn[*,‡,§]

[†]WACKER-Institut für Siliciumchemie, [‡]Chair of Inorganic Chemistry, [§]Molecular Catalysis, Catalysis Research Center, Department of Chemistry, Technische Universität München, Lichtenbergstrasse 4, 85747 Garching b. München, Germany

Supporting Information

ABSTRACT: A detailed study investigating the mechanism of the hydrosilylation of 4-F-acetophenone by *N*-heterocyclic biscarbene rhodium(I) complexes was performed, delivering substantial experimental evidence for a recently proposed catalytic cycle and explaining the observed side-product formation. Labeling experiments, silylene trapping reactions, and specific catalytic reactions were employed to substantiate each step of the catalytic cycle and explain the differences observed for different types of chiral catalysts. It is further shown that hydrosilylation and dehydrocoupling reactions with dihydrosilanes are mechanistically related.

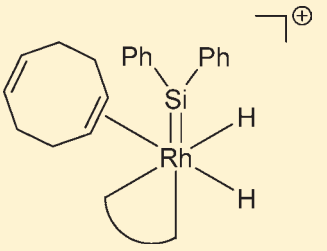

INTRODUCTION

Rhodium complexes are commonly used catalysts for the hydrosilylation of ketones.[1] Although the reaction is well established, only a few mechanistic studies on rhodium-based hydrosilylation reactions have been published.[2] Based on their investigations on Wilkinson's catalyst in the hydrosilylation of ketones, Ojima et al. proposed a mechanism shown in Scheme 1, which will be further addressed as the *Ojima mechanism*.[2a,2b]

In the first step of this mechanism, a Rh(III) species is formed via oxidative addition of the silane R_3SiH ($\mathbf{I^O}$). Then a ketone coordinates to the metal center ($\mathbf{II^O}$) before it inserts into the Rh−Si bond to form a Rh(III) alkyl hydride species ($\mathbf{III^O}$). These steps are followed by reductive elimination to yield the product ($R^1R^2CH-O-SiR_3$) and regenerate the catalyst L_nRh ($\mathbf{IV^O}$).

The isolation of $[RhClH(SiEt_3)(PPh_3)_2]$ provided experimental evidence for the existence and formation of the first intermediate of this catalytic cycle.[2a] Experimental results obtained by replacement of monohydrosilanes by dihydrosilanes, however, do not support the Ojima mechanism. Considerable rate enhancement was observed, and the product selectivities for the hydrosilylation of α,β-unsaturated ketones differ significantly for mono- and dihydrosilanes (1,4- versus 1,2-addition).[2a,2c] A kinetic isotope effect of two (KIE = 2) was determined in case of dihydrosilanes, which—along with the above-described differences—led to the proposal of a different mechanism for the hydrosilylation of ketones with dihydro- and trihydrosilanes by Zheng and Chan,[2c] while the Ojima mechanism is still accepted for the use of monohydrosilanes. The *Zheng mechanism* is depicted in Scheme 2.

After the initial oxidative addition of the silane R_2SiH_2 to the Rh(I) complex L_nRh ($\mathbf{I^Z}$), a ketone is thought to coordinate to the silicon atom ($\mathbf{II^Z}$) and then to insert into the Si−H bond forming a rhodium silyl hydride complex ($\mathbf{III^Z}$). In the last step,

Scheme 1. Ojima Mechanism[2a,2b]

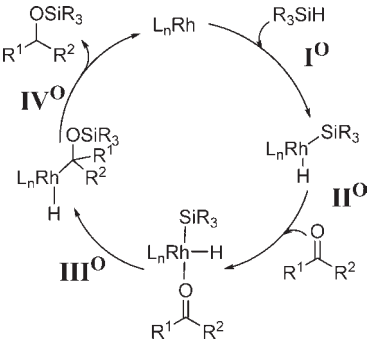

reductive elimination generates the product $R^1R^2CH-O-SiR_2H$ and recovers the catalyst ($\mathbf{IV^Z}$).

Recently, Gade et al. reported on the enantioselective hydrosilylation of ketones catalyzed by a Rh(I) complex bearing a chelating chiral NHC−oxazoline ligand.[3] In addition to the aforementioned rate enhancement for dihydrosilanes versus monohydrosilanes they determined an inverse kinetic isotope effect, which cannot be explained by either of the two mechanisms described above. Therefore a third, silylene-based mechanism was proposed (Scheme 3) for the hydrosilylation with dihydrosilanes, supported by a theoretical study comparing the three mechanisms.[2d,2e] According to the calculations of Gade et al.,[2e] the *Gade mechanism* involves the lowest activation barrier for the rate-determining step.

Whereas the first step ($\mathbf{I^G}$) is consistent with both mechanisms discussed above ($\mathbf{I^O}$ and $\mathbf{I^Z}$), the second step involves the transfer

Received: November 8, 2010
Published: December 27, 2010

   dx.doi.org/10.1021/ja110017c | *J. Am. Chem. Soc.* 2011, 133, 1589–1596

Scheme 2. Zheng Mechanism[2c]

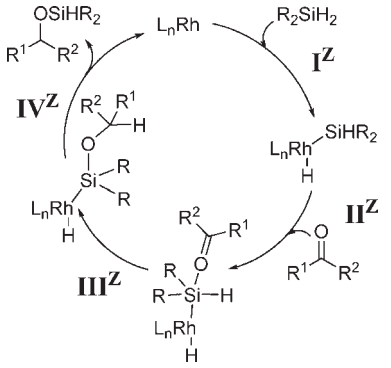

Scheme 3. Gade Mechanism[2d,2e]

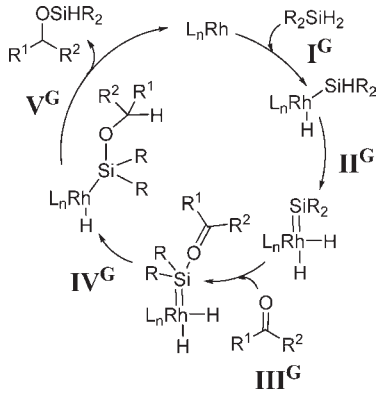

Scheme 4. Indirect Proof of a Rhodium Silylene Species by Milstein et al.[5]

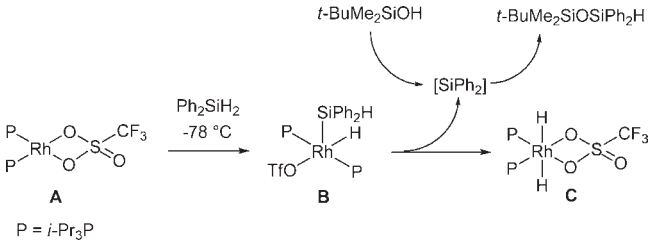

of the second hydrogen atom from the silyl ligand to the rhodium center and thus the formation of a silylene rhodium dihydride species ($\mathbf{II}^{\mathbf{G}}$). The ketone then coordinates to the electron-deficient silicon atom ($\mathbf{III}^{\mathbf{G}}$). After that a hydride is transferred from the metal to the carbonyl carbon atom ($\mathbf{IV}^{\mathbf{G}}$). The catalytic cycle is closed by reductive elimination of the product ($\mathbf{V}^{\mathbf{G}}$).

The existence of such a silylene species was discussed earlier in connection with rhodium-catalyzed dehydrogenative coupling reactions.[4] Goikhman and Milstein were the first to prove the presence of a rhodium silylene species by reacting a diphosphine rhodium triflate complex (**A**) with a stoichiometric amount of diphenylsilane.[5] Since the silylene species could not be directly observed, it was trapped with *t*-$BuMe_2SiOH$, while the corresponding rhodium dihydride complex **C** was isolated (Scheme 4).

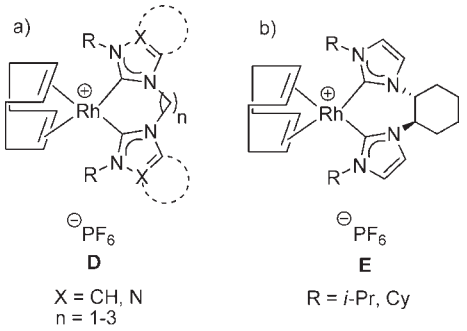

Figure 1. (a) Nonchiral and (b) chiral rhodium biscarbene complexes.

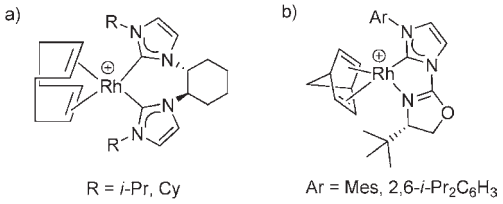

Figure 2. Chiral biscarbene complex **E** (a) and Gade's catalyst (b).

It was found that dehydrogenative coupling occurs when an excess of dihydrosilane is added to **A** but not if monohydrosilanes are employed instead. If stoichiometric amounts of styrene and silane are reacted with **A**, hydrogenation prevails over hydrosilylation, while hydrosilylation takes place under catalytic conditions. In the past decade, Tilley et al. isolated various metal—silylene species,[6] but to the best of our knowledge no rhodium silylene complex has yet been isolated.

Recently, we reported on a series of rhodium biscarbene complexes **D**, depicted in Figure 1a.[7] It was shown that the modification of the biscarbene ligand with respect to the composition of the heterocycle, the N-substituent, and the bridging group significantly effects the catalytic activity and product selectivity in the hydrosilylation of 4-F-acetophenone with diphenylsilane. In all cases, the formation of relatively high amounts of silylenolether was observed as side product.[7] The analogous chiral rhodium complexes **E** (Figure 1b), which were synthesized as described in the Supporting Information, do not lead to significant asymmetric induction in the hydrosilylation of 4-F-acetophenone, not even at low temperatures. This is surprising, because the very similar systems described by Gade et al. are highly enantioselective (Figure 2).[3]

In order to understand these differences, we carried out a detailed experimental study of the mechanism (*vide infra*). It provides strong experimental evidence for the existence of an intermediate silylene species and confirms the mechanism proposed by Gade et al., extending it by revealing further information on the side-product formation.

EXPERIMENTAL SECTION

General Remarks. All manipulations were carried out under a dry argon atmosphere using standard Schlenk techniques. Solvents were dried by standard methods[8] and distilled under nitrogen. ^{1}H, ^{2}H, ^{13}C, ^{19}F, and ^{29}Si NMR spectra were recorded on a JEOL JMX-GX 400 MHz and a Bruker Avance III 400 MHz spectrometer at room temperature and referenced to the residual solvent signal[9] or to TMS (^{29}Si). Spectral assignments were achieved by combination of ^{13}C DEPT, $^{1}H—^{13}C$

dx.doi.org/10.1021/ja110017c | J. Am. Chem. Soc. 2011, 133, 1589–1596

Scheme 5. Catalyst (1) and Catalytic Reaction

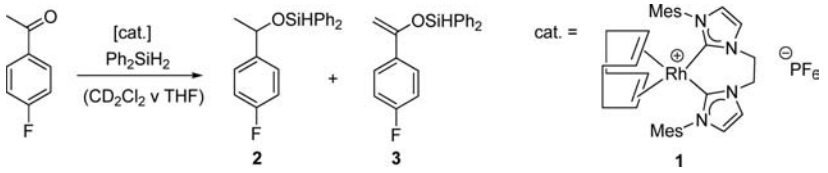

HMQC, and $^1H-^{13}C$ HMBC experiments. IR spectra were acquired using a Mettler-Toledo *react*IR spectrometer equipped with a fluid cell. GC/MS measurements were performed on a Varian CP-3800 gas chromatograph equipped with a 1200 L Quadrupol MS/MS and a HP 6890 GC system with a HP 597 mass selective detector. Compound **1** was prepared following an earlier published method.[7]

NMR Scale Stoichiometric Hydrogenation Reaction. A NMR tube was equipped with 8.5 mg (11.3 μmol) of **1**, silane (11.3 μmol), and 0.5 mL of CD_2Cl_2, and the reaction was monitored by ^1H NMR and ^{13}C NMR spectroscopy. NMR data of cyclooctane: ^1H NMR (CD_2Cl_2, 400 MHz) δ 1.53 (s, 16H); ^{13}C NMR (CD_2Cl_2, 100 MHz) δ 27.2 (s). NMR data of hydrogen: ^1H NMR (CD_2Cl_2, 400 MHz) δ 4.59 (s).

NMR Scale Catalytic Hydrogenation Reaction. In a typical experiment, a NMR tube was equipped with 6.8 mg (9.01 μmol) of **1**, olefin (0.45 mmol), silane (0.68 mmol), and 0.25 mL of CD_2Cl_2, and the reaction was monitored by ^1H NMR and ^{13}C NMR spectroscopy.

NMR Scale Scrambling Reaction. In a typical experiment, a NMR tube was equipped with 6.8 mg (9.01 μmol) of **1**, evacuated in a Schlenk flask, and refilled with D_2. Then, silane (0.45 mmol) and 0.5 mL of CD_2Cl_2 were added, and the reaction was followed by ^1H NMR spectroscopy.

Diphenylsilane-HD. To a solution of 1.11 g (5.11 mmol) of chlorodiphenylsilane in 10 mL of Et_2O was added dropwise 6.13 mL of $LiAlD_4$ (6.13 mmol, 1 M in Et_2O). The reaction mixture was stirred for 16 h at room temperature and then added to 10 mL of HCl (1 M aqueous solution). The organic phase was extracted with 10 mL of saturated NaCl solution, dried over Na_2SO_4, and filtered, before the solvent was removed in vacuo. The crude product was purified by bulb-to-bulb distillation (150 °C, 14 mbar) to afford 0.96 g (100%) of diphenylsilane-HD as a colorless liquid. ^1H NMR (C_6D_6, 400 MHz): δ 5.08 (s, 1H, Si-*H*), 7.10−7.14 (m, 6H, Ar-*H*), 7.51 (d, $^3J_{HH}$ = 7.0 Hz, 4H, Ar-*H*). ^{13}C NMR (C_6D_6, 100 MHz): δ 128.5 (s, Ar-*C*), 130.1 (s, Ar-*C*), 131.7 (s, Ar-*C*), 136.1 (s, Ar-*C*). ^2H NMR (C_6D_6, 61 MHz): δ 5.09 (s, 1H, Si-*D*). ^{29}Si NMR (C_6D_6, 79 MHz): δ −33.6 (t, $^1J_{SiD}$ = 30.3 Hz). Anal. Calcd for $C_{12}H_{11}DSi$ (185.32): C, 77.77; H, 7.07; Si, 15.16. Found: C, 78.00; H, 6.61; Si, 15.86.

NMR Scale Catalytic Hydrosilylation Reactions. In a typical experiment, a NMR tube was equipped with 6.8 mg (9.01 μmol) of **1**, 55 μL (62.2 mg, 0.45 mmol) of 4-F-acetophenone, silane (0.68 mmol), and 0.25 mL of CH_2Cl_2, and the reaction was monitored by ^{19}F NMR spectroscopy.

NMR Scale Trapping Reaction. To 4.1 mg (5.40 μmol) of **1** dissolved in 0.5 mL of CD_2Cl_2, 50 μL (50.1 mg, 0.27 mmol) of Ph_2SiH_2 and 43 μL (36.1 mg, 0.27 mmol) of *t*-$BuMe_2SiOH$ were added, and the reaction monitored by ^1H NMR and ^{29}Si NMR spectroscopy. NMR data of *t*-$BuSiMe_2-O-SiHPh_2$: ^1H NMR (CD_2Cl_2, 400 MHz) δ 0.08 (s, 6H, $SiCH_3$), 0.90 (s, 9H, CCH_3), 5.53 (s, 1H, Si*H*), 7.36 (m, 6H, Ar-*H*), 7.59 (m, 4H, Ar-*H*); ^{29}Si NMR (CD_2Cl_2, 79 MHz) δ −22.5 (s, Ph_2HSiO), 15.0 (s, *t*-$BuMe_2SiO$).

Determination of the KIE. To 3.0 mg (3.98 μmol) of **1** dissolved in 1.5 mL of dichloroethane, 24.5 μL of 4-F-acetophenone was added (27.7 mg, 0.20 mmol) and a 1:1 mixture of 41 μL of Ph_2SiH_2 (40.7 mg, 0.22 mmol) and 41 μL of Ph_2SiD_2 (41.1 mg, 0.22 mmol). The reaction was then followed by an *in situ* IR measurement. Ph_2SiH_2: IR (cm^{-1}) $\nu\sim_{SiH}$ 2148. Ph_2SiD_2: IR (cm^{-1}) $\nu\sim_{SiD}$ 1559.

Scheme 6. Proposed Mechanism

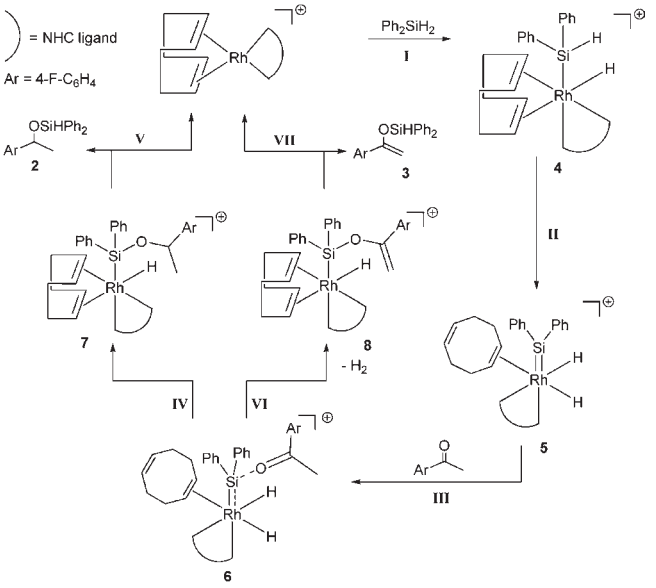

RESULTS

For the mechanistic investigations, [Rh(COD)(bis-NHC)]-[PF_6] with R = Mes, X = CH, and n = 2 (**1**) was chosen due to its comparatively high activity and selectivity.[7] Compound **1** and the catalytic model reaction are shown in Scheme 5.

4-F-Acetophenone was selected as the substrate because it offers the possibility to monitor the reaction progress by ^{19}F NMR spectroscopy. In all ^1H, ^{13}C, ^{19}F, and ^{29}Si NMR and IR spectra, no direct evidence for a Rh(III) species was found; within the time scales of these methods, only the original complex and the evolving products are observable. The results of various experiments, which indirectly prove the silylene-based mechanism depicted in Scheme 6, are discussed in the following paragraphs.

Steps **I**−**V** involving the intermediates **4**−**7** correspond to the Gade mechanism. An alternative pathway that leads to the formation of silylenolether **3**, the byproduct observed in the hydrosilylation reaction, is represented by the steps **VI** and **VII**. It requires the ketone in the intermediate **6** to tautomerize to its enol form under formation of silyl complex **8** and the release of hydrogen (step **VI**, Scheme 6). By reductive elimination of **3**, the catalytically active species is regenerated in step **VII**. Each elementary step (**I**−**VII**) of the mechanism was investigated by specific experiments, which will be discussed in detail below.

Oxidative Addition (I). In the first step, the silane adds oxidatively to the cationic Rh(I) center. As mentioned above, no Rh(III) species nor any color change can be observed by NMR, IR, or UV−vis spectroscopy. In order to understand how

dx.doi.org/10.1021/ja110017c | *J. Am. Chem. Soc.* 2011, 133, 1589–1596

Scheme 7. Reaction Pathways of 1 in Absence of Substrate

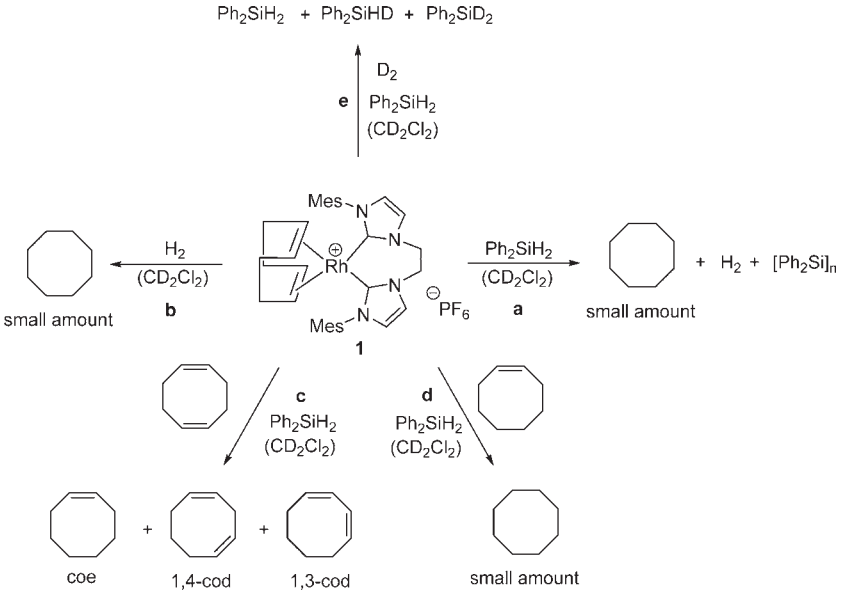

Scheme 8. Formation of 9, 10, and 11

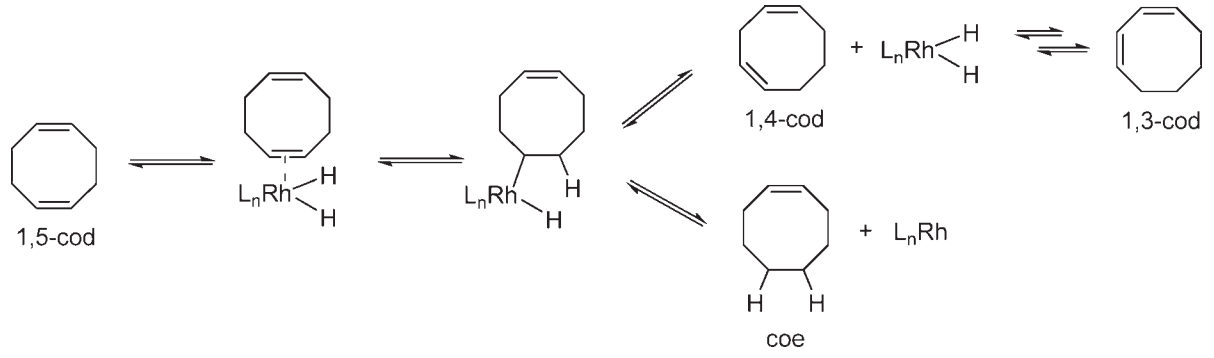

the silane reacts with **1** in absence of the ketone, the reactions **a**−**e**, shown in Scheme 7, were examined.

If stoichiometric amounts of diphenylsilane are reacted with **1** (reaction **a**, Scheme 7), a small amount of cyclooctane evolves after several hours, giving rise to a singlet in the ^{1}H and ^{13}C NMR spectrum at 1.53 and 27.2 ppm, respectively. A GC−mass spectrum confirms the formation of cyclooctane. Besides, hydrogen was detected by its characteristic signal at 4.59 ppm in the ^{1}H NMR spectrum. Simultaneously, a strong broadening of the aromatic signals in the ^{1}H and ^{13}C NMR spectra was observed, indicating an oligomeric diphenylsilane species, which is typical for rhodium-catalyzed dehydrogenative coupling reactions.[4,10]

Hydrogenation of the ligand also occurs when **1** reacts with hydrogen in dichloromethane (reaction **b**, Scheme 7). Addition of equimolar amounts of 1,5-cyclooctadiene (1,5-cod) and diphenylsilane to a solution of 2 mol % catalyst in dichloromethane leads to the formation of cyclooctene (coe) and the 1,4- and 1,3-isomers of cyclooctadiene (reaction **c**, Scheme 7), which can be explained with an interplay of M−H insertion and β-H-elimination reactions (Scheme 8).

The products were identified by ^{1}H and ^{13}C NMR spectroscopy (Table 1, entries 1−3) and GC−mass spectrometry (1,5-cod (m/z 108), 1,4-cod (m/z 108), 1,3-cod (m/z 108), and coe (m/z 110)).[11]

In contrast to the conditions applied under **a**, complete hydrogenation of the cyclooctadiene is not observed in the case of **c**. This is attributed to the chelating effect of the excess 1,5-cyclooctadiene. After hydrogenation of the first double bond, regeneration of the chelate complex is favored over hydrogenation of the second double bond. If cyclooctene is employed as substrate, a small amount of cyclooctane is formed very slowly (several days) (reaction **d**, Scheme 7).

In order to prove an intermediate existence of a dihydride species, diphenylsilane is reacted with 2 mol % of **1** under a D_2 atmosphere (reaction **e**, Scheme 7). For that case, formation of Ph_2SiD_2 and H_2 is expected, since the dihydride could be substituted by reductive elimination of hydrogen and subsequent oxidative addition of deuterium (Scheme 9).

A complete HD scrambling at the diphenylsilane moiety can be observed in the ^{1}H and ^{2}H NMR spectra, similar to the investigations of Comte et al. with their [(*o*-dppbe)Rh(COD)](OTf) system.[13] The appearance of Ph_2SiHD can be attributed to a HD exchange at **4** or the reaction of **5** with Ph_2SiD_2 (or *vice versa*) (Scheme 9).

dx.doi.org/10.1021/ja110017c |*J. Am. Chem. Soc.* 2011, 133, 1589–1596

Table 1. Characteristic NMR Signals of coe, 1,4-cod, and 1,3-cod in CD_2Cl_2[12]

entry	compound	selected ^{1}H NMR shifts (multiplicity, integral), ppm	selected ^{13}C NMR shifts, ppm
1	cyclooctene	1.49, 2.13	26.0, 26.7, 29.8
2	1,4-cyclooctadiene	1.41 (quin, 2H), 2.27 (quar, 4H), 2.79 (t, 2H)	23.5, 25.3, 29.9
3	1,3-cyclooctadiene	1.50[a], 2.17[a]	23.7, 28.6
4	[5-^{2}H$_1$]-cyclooctene	covered by coe	25.9, 26.0, 26.3 (t, $^1J_{HD}$ = 19.1 Hz), 26.6, 29.7
5	[6-^{2}H$_1$]-1,4-cyclooctadiene	covered by cod	23.4, 24.9 (t, $^1J_{HD}$ = 19.8 Hz), 25.2, 29.6

[a] Covered by signal of coe; visible only in 2D spectra.

Scheme 9. HD-Scrambling of Ph_2SiH_2 under D_2 Atmosphere

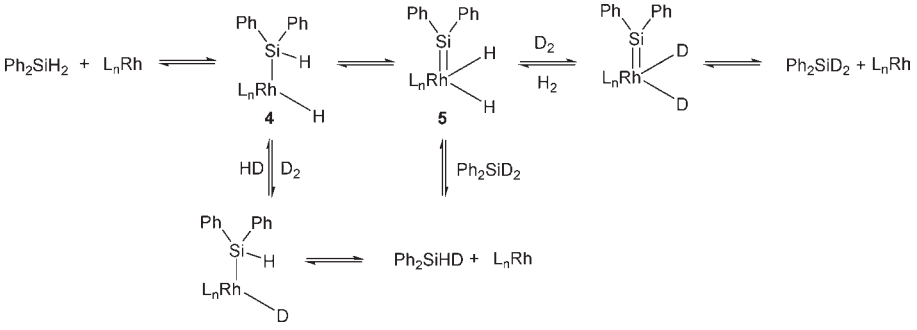

Scheme 10. Possible Intermolecular Reaction Pathway to a Rhodium Dihydride Species (Curtis−Epstein Mechanism)[14]

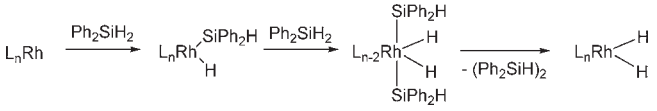

All of the discussed experiments (reactions **a**−**e**, Scheme 7) did not proceed in the absence of **1**. These findings support the formation of the intermediate rhodium dihydride complex **5** (Scheme 6), which is analogous to the one Goikhman and Milstein reported.[5] Hence, an oxidative addition as the first step of the mechanistic cycle, as it is proposed in all other mechanisms described so far, is evident, since it is necessary to explain the hydrogenation and scrambling behavior, which only occurred in presence of **1**. The rhodium dihydride can subsequently be formed by an intramolecular (as proposed) or an intermolecular process, which will be discussed in the following section.

α-H Transfer (II). In the key step of the mechanistic cycle, it was proposed[2d,2e] that a second silicon-bonded hydrogen atom is transferred to the metal center affording the silylene rhodium dihydride species **5**. To prove the formation of **5** and exclude an intermolecular reaction pathway[14] (Scheme 10), it is necessary to show that both hydrogen atoms involved in the reduction of 1,5-COD (reaction **c**, Scheme 7) originate from one molecule of diphenylsilane.

Therefore Ph_2SiHD was synthesized and reacted with an equimolar amount of 1,5-cyclooctadiene using 2 mol % of **1**, with the expectation to give different product distributions for intra- and intermolecular reaction pathways. Scheme 11 shows the five main products of the reaction.

Besides the formation of coe (**9**), 1,4-cod (**10**), and 1,3-cod (**11**), two deuterated products appear in the ^{13}C NMR. Their formation can be attributed to [5-^{2}H$_1$]-coe (**12**) and [6-^{2}H$_1$]-1,4-cod

Scheme 11. Hydrogenation of cod with Ph_2SiHD

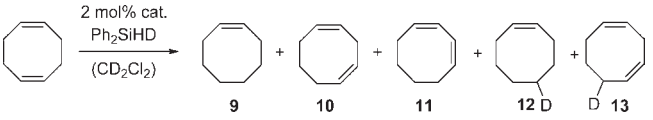

(**13**) and was confirmed by their characteristic masses of m/z 111 for **12** and 109 for **13**. Selected ^{13}C signals for **12** and **13** are shown in Table 1 (entries 4 and 5). Both compounds show the characteristic triplet pattern for the deuterium-bound carbon atom with the corresponding $^1J_{CD}$ coupling constant of about 20 Hz. The product distribution corresponds to an intramolecular hydrogenation transfer as depicted in Scheme 12.

Coordinated 1,5-cyclooctadiene can insert either into the Rh−H (**F**) or Rh−D (**G**) bond to form an intermediate alkyl rhodium hydride/deuteride complex. Subsequently, the complex can undergo reductive elimination to **12** or β-hydride elimination either to 1,5-cod, **13**, [5-^{2}H$_1$]-1,5-cyclooctadiene (**14**), or **10**. In the first step, insertion into the Rh−D bond should be thermodynamically favored, due to the stronger C−D versus C−H bond, and for the same reason β-hydride elimination should favor the formation of the deuterated compounds **12** and **13**. The resulting rhodium dihydride complex can then give rise to the formation of **9**, **10**, and **11**, as well as reaction pathway **G** (cp Scheme 8). Compound **14** cannot be identified in the ^{13}C NMR spectrum due to the overlapping signals of excess cod. ^{2}H NMR and GC−mass, however, provide evidence for the presence of this compound. Hence, this experiment supports the assumption of two subsequent intramolecular hydrogen transfers from the silicon atom to the metal center by reacting **1** with diphenylsilane. In the case of an intermolecular reaction pathway, an intermediate rhodium bisdeuterated species should occur and result in DD-hydrogenation products (Scheme 13).

dx.doi.org/10.1021/ja110017c | J. Am. Chem. Soc. 2011, 133, 1589–1596

Scheme 12. Possible Reaction Network for the Hydrogenation of cod with Ph_2SiHD

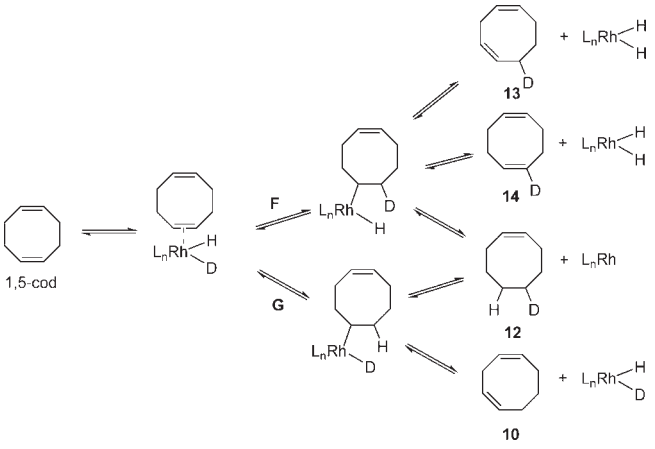

Scheme 13. Rhodium Dideuteride Complex by an Intermolecular Reaction Pathway

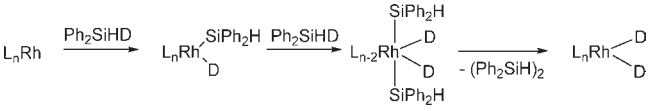

Based on these results, the reaction of a catalytic amount of **1** with diphenylsilane very likely leads to a highly reactive silylene species **5**. The formation of an oligomeric silane species in the absence of substrate can be explained by the reaction of this silylene species with another molecule of silane, as it has been proposed earlier.[4] The existence of such an accordant silylene species in the presence of substrate was investigated and will be discussed in the following section.

Monohydrosilanes, in contrast to dihydrosilanes, cannot undergo the second hydrogen transfer (**II**, Scheme 6), and thus pronounced differences are expected for the catalytic reaction. Therefore the hydrosilylation of ketones with the dihydrosilanes Ph_2SiH_2 and $PhMeSiH_2$ and the monohydrosilane Ph_2MeSiH in the presence of catalytic amounts of **1** was investigated. In accordance to other studies,[2a−2d] the use of monohydrosilane reduces the reaction rate by several orders of magnitude (Ph_2MeSIH, TOF < 0.1 h^{-1}) as compared with dihydrosilanes (**1**, TOF = 150 h^{-1}) (Figure 3). The monohydrosilane, however, does not produce any byproduct **3**.

The rate enhancement using dihydrosilanes could be explained with both the Zheng mechanism (step **III**$^{\mathbf{Z}}$ in Scheme 2) and the silylene-based Gade mechanism. To determine which of the mechanisms is valid in our case, a typical silylene trapping experiment was performed. *t*-$BuMe_2SiOH$ is known to react with a silylene species by forming a disiloxane (see Scheme 4), which is easy to characterize by ^1H and ^{29}Si NMR spectroscopy.[5] Due to its steric bulk, side reactions are minimized and coordination to the metal center can be excluded. Therefore a catalytic amount of complex **1** (2 mol %) was dissolved in dichloromethane, and equimolar amounts of diphenylsilane and *t*-$BuMe_2SiOH$ were added, while ^1H and ^{29}Si NMR spectroscopy were employed to monitor the reaction progress. Upon contact of the reaction partners, vigorous gas evolution was observed, and formation of

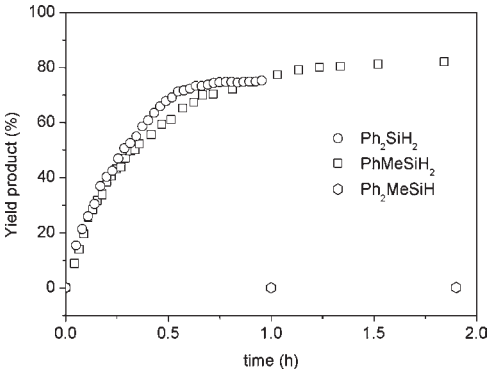

Figure 3. Different reactivity of secondary and tertiary silanes.

Scheme 14. Trapping Experiment with *t*-$BuMe_2SiOH$ and the Possibly Involved Reaction Pathways

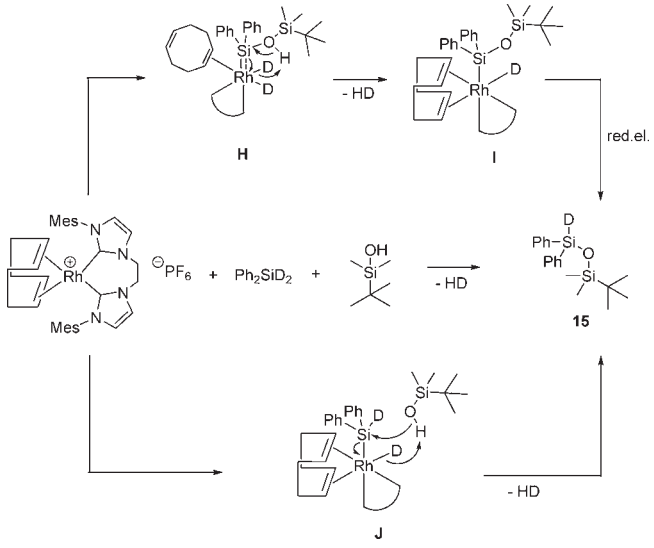

H_2 was detected by ^1H NMR spectroscopy. Simultaneously, the signals of Ph_2SiH_2 (−33.5 ppm) and *t*-$BuMe_2SiOH$ (19.4 ppm) decrease in the ^{29}Si NMR spectrum and two new signals arise at 15.0 ppm and −22.5 ppm, which are assigned to the quantitatively formed disiloxane **15**. The same reaction using Ph_2SiD_2 instead, leads to formation of HD and exclusive deuteration at the diphenylsilane moiety, with its characteristic Si−D signal at 5.52 ppm in the ^2H NMR spectrum (Scheme 14).

The reaction can occur via two possible reaction pathways (Scheme 14). According to the Gade mechanism, the silanol coordinates to the electron-deficient silylene Si atom of **H**, the silyl complex **I** and H_2 are formed, and **15** is generated by reductive elimination. Alternatively, the silanol may react with the silyl rhodium(III) hydride complex **J** in a concerted mechanism. In the latter case, no significant differences in reactivity using mono- or dihydrosilanes would be expected. However, while the reaction with Ph_2SiH_2 is completed within 1 h, no conversion of the monohydrosilane takes place over a period of several days. Consequently, intermolecular interactions can be ruled out, and a second Si-bound hydrogen atom is required to explain the observed reactivity. These considerations thus serve as an indirect proof for the existence of a silylene rhodium(III) dihydride as key

dx.doi.org/10.1021/ja110017c |*J. Am. Chem. Soc.* 2011, 133, 1589–1596

Table 2. Yields of Product (2) and Byproduct (3) for Various Reaction Conditions Involving Electronically Different Silanes

silane	solvent	product yield (**2**) (%)	byproduct yield (**3**) (%)
Ph_2SiH_2	CD_2Cl_2	68	32
Ph_2SiH_2	THF	74	26
$PhMeSiH_2$	CD_2Cl_2	84	16
$[(o\text{-OMe})Ph]_2SiH_2$	CD_2Cl_2	92	8

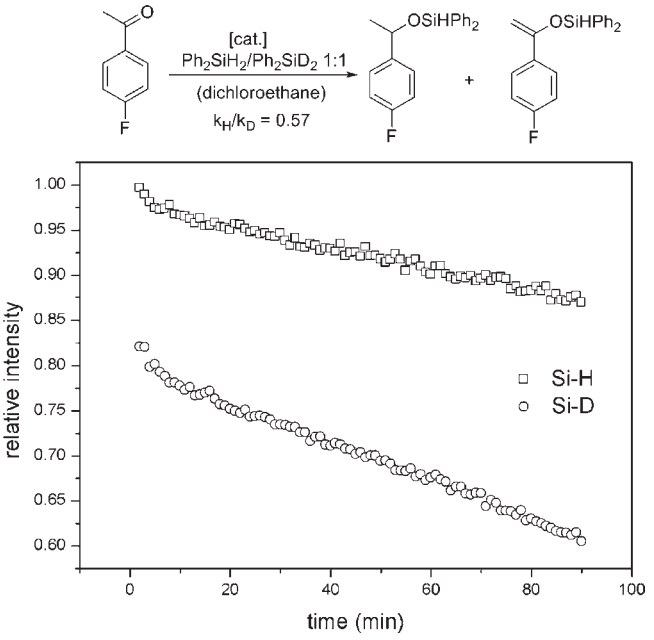

Figure 4. Determination of the inverse KIE.

intermediate of the mechanistic cycle. Any attempts to stabilize **5** by using electron-donating di(2-methoxyphenyl)silane,[15] sterically hindered dimesitylsilane, or a NHC ligand with coordinating N-substituents were not successful, not even when carried out at low temperatures.

Product and Side-Product Formation (IV−VII). As an effect of the Lewis acidity of the silylene Si atom, the ketone coordinates to the silicon atom instead of the rhodium center (**III**, Scheme 6). After coordination to the silicon atom, two possible reaction pathways arise, as discussed earlier. The driving force for the formation of the undesired silylenolether **3** is the evolution of hydrogen (**VI**, Scheme 6). This reaction pathway can be suppressed by performing the reaction under H_2 pressure as Comte et al. showed for the analogous $[(o\text{-dppbe})Rh(COD)](OTf)$ system.[16] Another approach is to reduce the Lewis acidity of the electron-deficient silicon atom, which would favor the keto tautomer **6**. For that purpose, THF as coordinating solvent and various silanes were tested under catalytic conditions. The resulting yields of **2** and **3** are summarized in Table 2.

Replacement of the noncoordinating solvent methylene chloride by the coordinating tetrahydrofurane resulted in a slight increase in product selectivity (68% → 74%). The same trend was observed when Ph_2SiH_2 was replaced by the more electron-rich $PhMeSiH_2$ (84%) or the *ortho*-methoxy-substituted diphenylsilane[15] (92%). These observations confirm the assumption that the Lewis

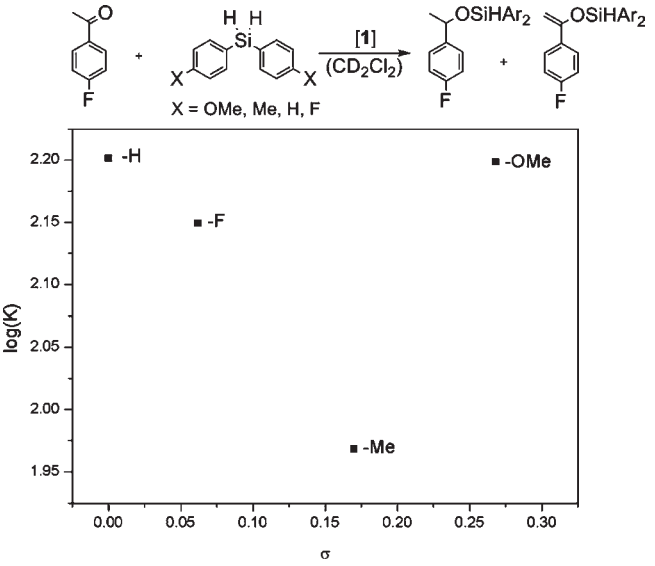

Figure 5. Hammet plot of the catalytic reaction using different *para*-substitued diephenylsilanes **16**.

acidity of the silylene silicon atom is responsible for the high amounts of side-product formation. Accordingly, the monohydrosilane Ph_2MeSiH, which cannot generate such a silylene species, does not produce any byproduct.

The ketones' coordination at the silicon atom results in a long distance interaction between the chiral information in $[Rh(COD)(bis\text{-}NHC)](PF_6)$ where bis-NHC = cyclohexyl-bridged imidazole-based biscarbene (Figure 2a) and the substrate. Consequently, low asymmetric induction is observed. The ligands used by Gade et al. (Figure 2b) are more flexible, and the chiral information is located closer to the reaction site, which could explain the better asymmetric induction reported.

Kinetic Isotopic Effect (KIE). All experiments discussed so far give experimental evidence for the silylene-based mechanism, first postulated by Gade and co-workers based on DFT calculations. Hydride transfer from the metal to the substrate was assigned as rate-determining step, explaining the observed inverse kinetic isotopic effect for their system.

In order to investigate this aspect for our system, catalysis was performed by the hydrosilylation reaction of 4-F-acetophenone with a mixture of Ph_2SiH_2 and Ph_2SiD_2 (1:1) in dichloroethane,[17] which was monitored by *in situ* IR spectroscopy. The change of the relative intensity of the Si−H versus Si−D band over time is represented in Figure 4.

The stronger decrease of the Si−D band results in an inverse kinetic isotope effect of $k_H/k_D = 0.57$, which Gade et al. attributed to the thermodynamically stronger C−D vs C−H bond, which is formed in step **IV** (Schemes 3 and 6).[2d] Additionally, the absence of a Hammett correlation[18] using different *para*-substituted silanes[15] (Figure 5) indicates that neither of the first two reaction steps is rate-determining. Otherwise the different electronic properties of **16** would influence the catalyst's activity in a linear way.

■ CONCLUSION

In summary, experimental evidence for the formation of an intermediate rhodium silylene species is given. This intermediate species is generated by two subsequent hydrogen transfers from the silane

dx.doi.org/10.1021/ja110017c |*J. Am. Chem. Soc.* 2011, 133, 1589–1596

to the metal, which is confirmed by several experiments, such as the catalytic hydrogenation in the absence of substrate, the different reactivity of mono- and dihydrosilanes, and trapping with t-BuMe$_2$SiOH. The experiments provide substantial evidence that the ketone interacts with the catalyst by coordinating to the electron-deficient silylene silicon atom. The resulting transition state cannot be significantly affected by the distant and rigid chiral ligand applied in this work, which explains the low enantioselectivity.

The silylene species opens up two alternative reaction pathways. Besides the formation of product, the Lewis acidity of the silicon atom competitively enables the formation of the enole tautomer leading to the nondesired silylenolether as side product. The inverse kinetic isotope effect observed by Gade et al. is confirmed by our experiments. Based on this and the absence of a Hammet correlation when using different *para*-substitued diphenylsilanes, the product formation can be assigned as rate-determining step.

The chiral biscarbene rhodium(I) complexes investigated here are not well suited for the asymmetric hydrosilylation of ketones with dihydrosilanes. The transfer of chiral information, however, could be induced by locating the chirality closer to the generated silylene silicon atom.

In addition to giving experimental evidence for a silylene-based mechanism, our studies provide an explanation for the formation of the side product and show the mechanistic connection between Rh(I)-catalyzed hydrosilylation and dehydrocoupling.

■ ASSOCIATED CONTENT

Supporting Information. Experimental procedures for the synthesis of **E**, as well as the Diamond plot of $\mathbf{E}^{Cy}$ and supplementary crystallographic data for $\mathbf{E}^{Cy}$ in CIF format. This material is available free of charge via the Internet at http://pubs.acs.org.

■ AUTHOR INFORMATION

Corresponding Author
wolfgangherrmann@ch.tum.de; fritz.kuehn@ch.tum.de

■ ACKNOWLEDGMENT

We are grateful for the financial support of the Wacker Chemie AG and thank Prof. Peter Härter for helpful discussions.

■ REFERENCES

(1) (a) Riant, O.; Mostefaï, N.; Courmarcel, J. *Synthesis* **2004,** 2943–2958. (b) Nishiyama, H.; Itoh, K., . In *Catalytic Asymmetric Synthesis* 2nd ed.; Iwao, O., Ed.; Wiley-VCH: New York, 2000; pp 111-143. (c) Ojima, I.; Li, Z.; Zhu, J., . In *The Chemistry of Organic Silicon Compounds*, Rappoport, Z, Apeloig, Y., Eds.; John Wiley & Sons, Ltd.: Chichester, 2003; pp 1687−1792.

(2) (a) Ojima, I.; Nihonyanagi, M.; Kogure, T.; Kumagai, M.; Horiuchi, S.; Nakatsugawa, K.; Nagai, Y. *J. Organomet. Chem.* **1975,** *94*, 449–461. (b) Ojima, I.; Kogure, T.; Kumagai, M.; Horiuchi, S.; Sato, T. *J. Organomet. Chem.* **1976,** *122*, 83–97. (c) Zheng, G. Z.; Chan, T. H. *Organometallics* **1995,** *14*, 70–79. (d) Schneider, N.; Finger, M.; Haferkemper, C.; Bellemin-Laponnaz, S.; Hofmann, P.; Gade, L. H. *Angew. Chem., Int. Ed.* **2009,** *48*, 1609–1613. (e) Schneider, N.; Finger, M.; Haferkemper, C.; Bellemin-Laponnaz, S.; Hofmann, P.; Gade, L. H. *Chem.—Eur. J.* **2009,** *15*, 11515–11529.

(3) Gade, L. H.; César, V.; Bellemin-Laponnaz, S. *Angew. Chem., Int. Ed.* **2004,** *43*, 1014–1017.

(4) (a) Ojima, I.; Inaba, S.-I.; Kogure, T.; Nagai, Y. *J. Organomet. Chem.* **1973,** *55*, C7–C8. (b) Chang, L. S.; Corey, J. Y. *Organometallics* **1989,** *8*, 1885–1893. (c) Rosenberg, L.; Fryzuk, M. D.; Rettig, S. J. *Organometallics* **1999,** *18*, 958–969. (d) Fryzuk, M. D.; Rosenberg, L.; Rettig, S. J. *Organometallics* **1991,** *10*, 2537–2539.

(5) Goikhman, R.; Milstein, D. *Chem.—Eur. J.* **2005,** *11*, 2983–2988.

(6) (a) Calimano, E.; Tilley, T. D. *J. Am. Chem. Soc.* **2008,** *130*, 9226–9227. (b) Turculet, L.; Feldman, J. D.; Tilley, T. D. *Organometallics* **2004,** *23*, 2488–2502. (c) Feldman, J. D.; Peters, J. C.; Tilley, T. D. *Organometallics* **2002,** *21*, 4065–4075. (d) Peters, J. C.; Feldman, J. D.; Tilley, T. D. *J. Am. Chem. Soc.* **1999,** *121*, 9871–9872. (e) Mitchell, G. P.; Tilley, T. D. *J. Am. Chem. Soc.* **1998,** *120*, 7635–7636. (f) Waterman, R.; Hayes, P. G.; Tilley, T. D. *Acc. Chem. Res.* **2007,** *40*, 712–719.

(7) Riederer, S. K. U.; Gigler, P.; Högerl, M. P.; Herdtweck, E.; Bechlars, B.; Herrmann, W. A.; Kühn, F. E. *Organometallics* **2010,** *29*, 5681–5692.

(8) Pangborn, A. B.; Giardello, M. A.; Grubbs, R. H.; Rosen, R. K.; Timmers, F. J. *Organometallics* **1996,** *15*, 1518–1520.

(9) Fulmer, G. R.; Miller, A. J. M.; Sherden, N. H.; Gottlieb, H. E.; Nudelman, A.; Stoltz, B. M.; Bercaw, J. E.; Goldberg, K. I. *Organometallics* **2010,** *29*, 2176–2179.

(10) Unfortunately, a GPC measurement was not successful due to the small molecular weights of the oligomers.

(11) Assignment of the signals was done by 2D-NMR spectroscopy, such as, HMBC, HMQC, and DEPT.

(12) (a) Penman, K. G.; Kitching, W.; Wells, A. P. *J. Chem. Soc., Perkin Trans. 1* **1991,** 721–726. (b) Anet, F. A. L.; Yavari, I. *J. Am. Chem. Soc.* **1977,** *99*, 6986–6991. (c) Anet, F. A. L.; Yavari, I. *Tetrahedron Lett.* **1975,** *16*, 1567–1570. (d) Tsarev, V. N.; Wolters, D.; Gais, H.-J. *Chem.—Eur. J.* **2010,** *16*, 2904–2915.

(13) Comte, V.; Balan, C.; Gendre, P. L.; Moise, C. *Chem. Commun.* **2007,** 713–715.

(14) Curtis, M. D.; Epstein, P. S., . In *Advances in Organometallic Chemistry*, Stone, F. G. A., West, R., Eds.; Academic Press: New York, 1981; Vol. 19, pp 213−255.

(15) Gigler, P.; Herrmann, W. A.; Kühn, F. E. *Synthesis* **2010,** *2010*, 1431–1432.

(16) Comte, V.; Balan, C.; Gendre, P. L.; Moise, C. *Chem. Commun.* **2007,** 713–715.

(17) Dichloroethane was used instead of dichloromethane, due to its lower vapor pressure, to exclude changes in concentration.

(18) Hammett, L. P. *J. Am. Chem. Soc.* **1937,** *59*, 96–103.